Title	Seismic Response of High-rise Building with Viscous Dampers considering Its Performance Decrement under Long-period Ground Motion using 3D Model
Authors	Daiki Sato, Xiyuan Liu
Citation	Proceedings of the 12th Pacific Structural Steel Conference, , ,
Pub. date	2019, 11

12th Pacific Structural Steel Conference
Tokyo, Japan, November 9 -11, 2019

SEISMIC RESPONSE OF HIGH-RISE BUILDING WITH VISCOUS DAMPERS CONSIDERING ITS PERFORMANCE DECREMENT UNDER LONG-PERIOD GROUND MOTION USING 3D MODEL

Daiki Sato*, Xiyuan Liu*

* Tokyo Institute of Technology, Yokohama, Japan
e-mails: sato.d.aa@m.titech.ac.jp, liu.x.ar@m.titech.ac.jp

Keywords: High-rise buildings, Viscous damper, Long-period ground motion, Performance decrement, 3D model

Abstract. *This study determined the seismic response of a 20-story building with viscous dampers, considering the performance decrement of the dampers under long-period ground motion, using three analysis methods (conventional, simplified, and detailed) and including story drift angle, absolute acceleration, absorbed energy of individual viscous dampers, absorbed energy of total viscous dampers, damping energy of structure, and energy distribution rate of dampers. The building is elastic and elasto-plastic. The analysis methods were also assessed. The simplified method is the most effective method. Two types of viscous dampers (medium-sized and large-sized) were evaluated using energy density and decrease rate. The performance decrement of large-sized dampers is less than that of medium-sized dampers. Also, the larger the number of dampers is, the lower the decrease rate is.*

1 INTRODUCTION

Long-period ground motions are expected to be generated by potential Nankai Trough earthquakes. These will attack the three major metropolitan areas of Japan: Tokyo, Osaka, and Nagoya. It is feared that high-rise buildings with long natural periods will be severely affected. The passive control device is effective against long-period ground motion. The viscous damper targeted in this study is a flow resistance type damper that uses the flow resistance force of the enclosed fluid. However, while vibration energy is converted into thermal energy, the temperature of the viscous fluid increases and the damper performance decreases. Therefore, a design method for the vibration control of buildings needs to include the performance decrement of viscous dampers under long-period ground motion.

The design of a structure with viscous dampers is based on time history and energy analyses [1]. Kasai et al.[2] performed long-term sinusoidal wave excitation tests on full-scale viscous dampers. They proposed a performance decrement evaluation method using energy density, in which the cumulative absorbed energy is divided by the volume of the viscous fluid. Nagayama et al.[3,4] proposed a simplified response evaluation method for the vibration control of a building with viscous dampers; this method considered the performance decrement caused by long-period cyclic loading. Sato et al.[5-6] assessed three analysis methods, the conventional, simplified, and detailed methods, and researched the decrease rate using the simplified method and the Multi Degree of Freedom Model (MDOF) model. The simplified method, which does not consider the cyclic decrease rate, is the most effective among the three method. Okada, R. and Sato, D.[7-8] examined the validity of the simplified method which considering the plasticity of the building structure using the MDOF model. The influence of the performance decrement of the dampers on the seismic response is smaller when the structure is elasto-plastic than when it is elastic. Moreover, they also researched the energy of passive structures with dampers and verified the accuracy of their energy distribution measurements using the MDOF model.

This paper presents the results of a study on the seismic response of a 20-story building with viscous dampers, considering the performance decrement of the dampers under long-period ground motion, using a 3D model. In section 2, the parameters of the viscous dampers and the building are presented. Based on the volume of the enclosed fluid, two types of dampers were adopted. The structure is elastic and elasto-plastic . Moreover, an analysis model for the viscous dampers, considering performance decrement and the distribution of the dampers, is proposed. In section 3, two input ground motions are presented. In section 4, three analysis methods, conventional, simplified, and detailed, were assessed using the seismic responses. In section 5, the decrease rate when the structure is elastic versus that when it is elasto-plastic is researched, including the absorbed energy of individual dampers, the decrease rate of two types of dampers, and the decrease rate corresponding to the three analysis methods.

2 SUMMARY OF DAMPERS AND THE BUILDING

2.1 Viscous Dampers

Based on the volume of the enclosed fluid, two types of viscous dampers, medium-sized and large-sized, were considered. The velocity index α and the viscous coefficient C_d of the viscous dampers are shown in Table 1[2]. Since the dampers and the support members are connected in series (Figure 1), the internal stiffness K_d and support member stiffness K_b can be shown using the equivalent stiffness (Table 1) K_b^*[5].

Table 1 Parameters of viscous dampers

object	α	V_V [mm^3]	C_d [kN·(s/mm)$^\alpha$]	K_d [kN/cm]	K_b [kN/cm]	K_d^* [kN/cm]
Medium-sized	0.38	8.34×10^6	98	2663	2525	1296
Large-sized	0.38	2.48×10^7	196	4858	4842	2425

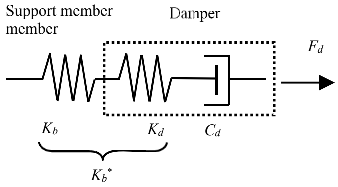

Figure 1 Damper and support member

2.2 Analysis Model Considering Performance Decrement of Viscous Dampers

The force of a viscous damper $F_d^{(n)}$ in step n, is expressed by Equation (1):

$$F_d^{(n)} = C_d^{(n)} \cdot \left|\dot{u}_d^{(n)}\right|^\alpha \operatorname{sgn}(\dot{u}_d^{(n)}) \tag{1}$$

where $\dot{u}_d^{(n)}$ is the velocity at step n; $C_d^{(n)}$ is the viscous coefficient at step n. $C_d^{(n)}$, considering its repeated effect, is calculated using Equation (2) [2]. The decrease rate $\lambda^{(n)}$ of the viscous coefficient due to the repeated effect of $C_d^{(n)}$ is defined by Equation (3) [2].

$$C_d^{(n)} = \lambda^{(n)} \cdot C_d^{(0)} \tag{2}$$

$$\lambda^{(n)} = \exp(-a_0 \cdot \Omega^{(n)}) \tag{3}$$

where $C_d^{(0)}$ is the initial value of the viscous coefficient and a_0 is the value depending on the standard of the damper, which can be calculated from a long-term excitation experiment. In this study a_0=1.695×10-6 m^2/kN[1]. $\Omega^{(n)}$ is the energy density at step n, which is described by Equation (4) [2]:

$$\Omega^{(n)} = \frac{w_d^{(n)}}{V_V} \tag{4}$$

where $w_d^{(n)}$ is the cumulative absorbed energy up to step n of the damper and V_V and is the volume of the viscous fluid. According to Table 1, the V_V of a medium-sized damper is 0.0083436 m^3, and the V_V of a large-sized damper is 0.024823712 m^3 [2].

Figure 2[2] presents the long-term excitation experiment results and analytical results. The period of the sinusoidal wave is 4.0 s, the amplitude of the sinusoidal wave is 20 mm. It can be verified that the analysis model can reproduce the tendency of the performance decrement with each cycle with high accuracy.

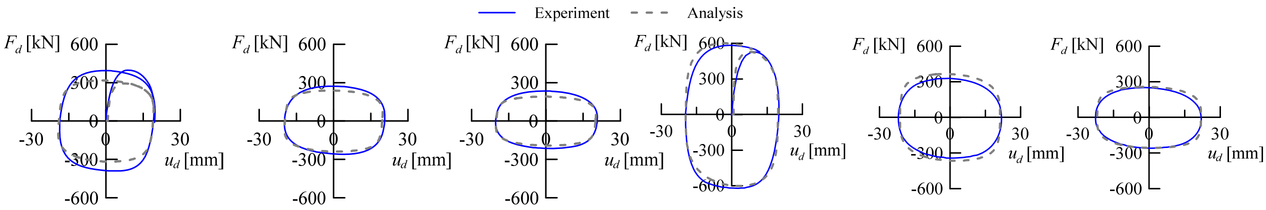

(i)1st Cycle (ii)75th Cycle (iii)114th Cycle (i)1st Cycle (ii)225th Cycle (iii)449th Cycle

(a) Medium-sized (T=4.0 s, u_d=20 mm) (b) Large-sized (T=4.0 s, u_d=20 mm)

Figure 2 Comparison between experimental and analysis results

2.3 Building Model

The height of the steel-frame building is 81.7 m, 20-stories [9]. The height upto the first floor is 6.0 m, the others are 4.0 m. Table 2 presents a column section list. To avoid the early yielding of the connection panel, the thickness of parts of the panel are made thicker than the thickness of the column. Table 3 presents the thickness of the panel. The long side direction of the structure is the X direction, and the short side direction is the Y direction. The X direction is considered. Figure 3 presents the plan and elevation of the building. The 1st and 2nd periods T_f (X direction) are 2.29 s and 0.81 s. Rayleigh damping is selected. The damping ratios for the 1st and 2nd modes are 1.5% and 1.95%. The structure is elastic and elasto-plastic. The shear force Q-drift angle R relationship is shown in Figure 4[10].

Table 2 Column list (mm)

Story	C1	C2	C3
17~20	550×550×25	500×500×22	500×500×19
13~16	600×600×28	550×550×25	500×500×19
9~12	650×650×28	600×600×28	550×550×22
6~8	650×650×32	600×600×28	600×600×25
4~5	700×700×32	650×650×28	650×650×28
2~3	750×750×36	700×700×36	700×700×32
1	800×800×36	750×750×36	750×750×32

Table 3 Panel list (mm)

Floor	C1	C2	C3
R~20	28	22	19
19~18	32	25	19
17~15	32	25	22
14~12	32	32	25
11~10	28	28	22
9~7	32	28	25
6~5	32	32	28
4~2	36	36	32

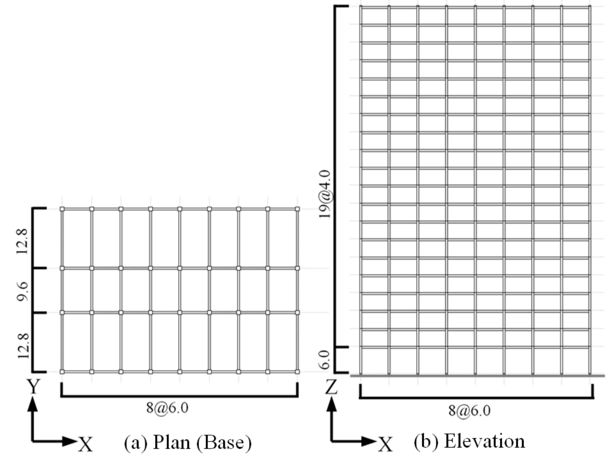

Figure 3 Plan and Elevation (m)

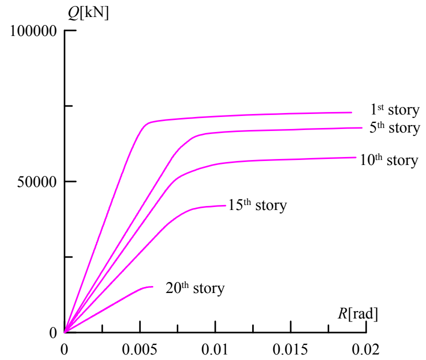

Figure 4 Relationship of shear force-drift angle

2.4 Distribution of Viscous Dampers

There are four types of damper distributions: $_{M}$R100、$_{L}$R100、$_{M}$R150、and $_{L}$R150. In addition, the medium-sized damper in Table 1 has the letter “M” to the left of its name, and large-sized damper similarly has the letter “L”. Under level 2 seismic ground motion (Art-Hachi), the story drift angle R of the structure with $_{M}$R100 and $_{L}$R100 is less than 1/100, and the story drift angle R of the structure with $_{M}$R150 and $_{L}$R150 is less than 1/150. Figure 5 presents the viscous coefficient in the height direction. Table 4 presents the number of viscous dampers in each story. Figure 6 to Figure 9 present the plan and elevation with dampers in the X direction.

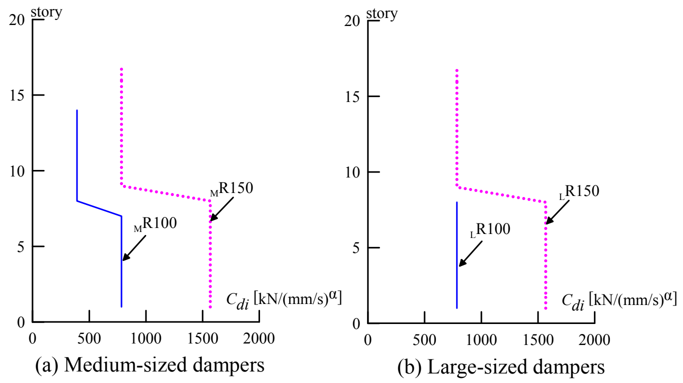

Figure 5 Viscous coefficient

Table 4 Number of viscous dampers

Story	$_{M}$R100	$_{M}$R150	$_{L}$R100	$_{L}$R150
18~20	0	0	0	0
15~17	0	8	0	4
9~14	4	8	0	4
8	4	16	4	8
1~7	8	16	4	8

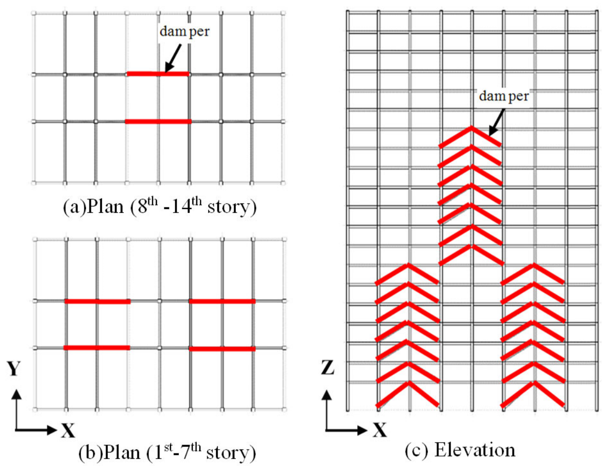

Figure 6 Plan and elevation with $_{M}$R100

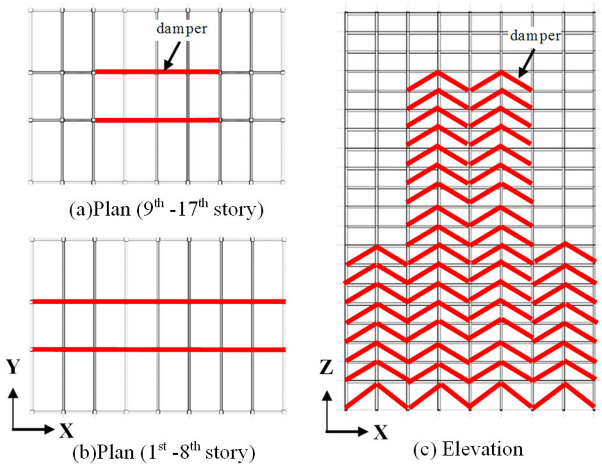

Figure 7 Plan and elevation with $_{M}$R150

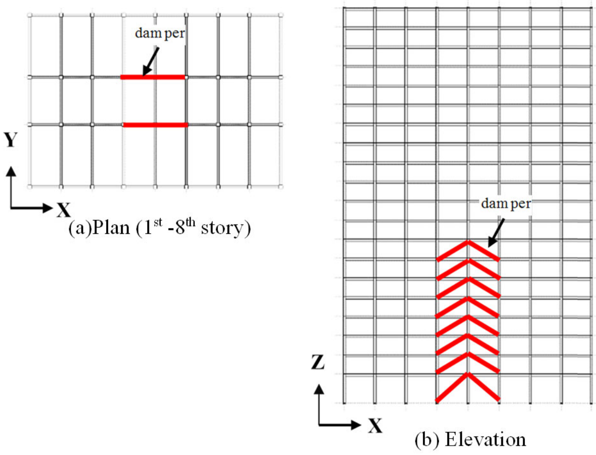

Figure 8 Plan and elevation with $_L$R100

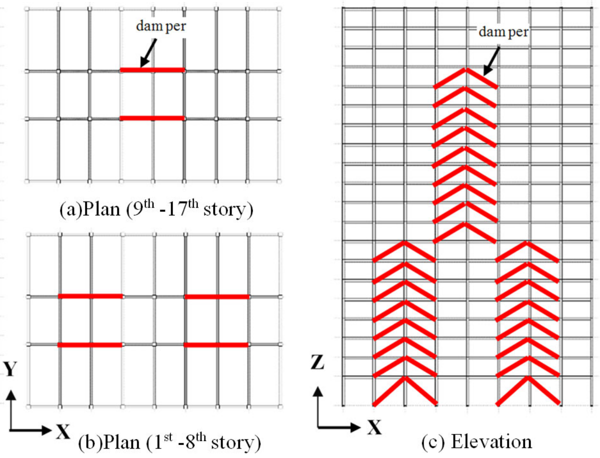

Figure 9 Plan and elevation with $_L$R150

3 INPUT GROUND MOTION

Two earthquakes were selected in this study: Art-Hachi (phase value: HACHINOHE 1968 EW), which is equivalent to an earthquake of level 2, and the long-period ground motion CH1 [11]. The S_v (h = 5 %) of level 2 is 100 cm/s after the corner period T_c=0.64 s. Figure 10 presents the acceleration of earthquakes. Figure 11 presents the pseudo-velocity response spectrum $_pS_v$ (h = 5 %) and energy spectrum V_E (h = 10 %). From Figure 11, it can be seen that the $_pS_v$ of CH1 is about 1.5 times larger than that of Art-Hachi; the V_E of CH1 is about 2.1 times larger than that of Art-Hachi.

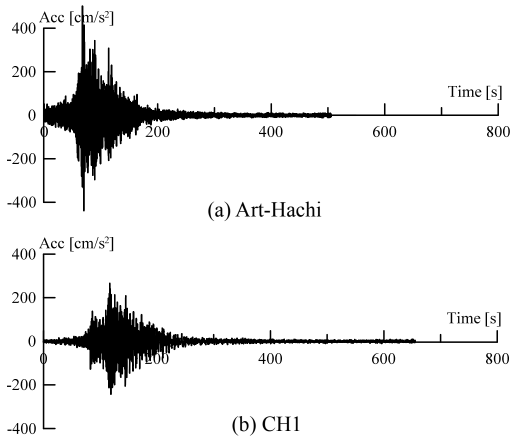

Figure 10 Acceleration of earthquake

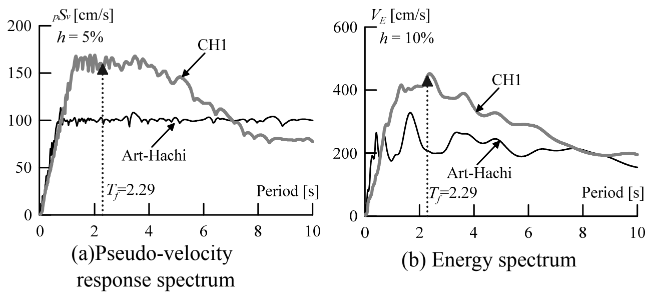

Figure 11 Response spectrum

4 TIME HISTORY RESPONSE ANALYSIS

Three analysis methods were used in the time history response analysis: conventional, simplified, and detailed. The conventional method uses the initial value of the viscous coefficient $C_d^{(0)}$ for analysis. The simplified method is based on the energy density Ω (Equation 4) of the conventional method, and the decrease rate λ can be calculated from the energy density Ω (Equation 3). After that, the initial value of the viscous coefficient $C_d^{(0)}$ is multiplied by the decrease rate λ (Equation 2), and the analysis is repeated using viscous coefficient C_d. Figure 12 presents the flowchart for the simplified method. The simplified method is valuable because the response evaluation is possible even when there is no analytical model for the characteristic value of the change of the viscous damper by repetition. The detailed method involves calculating the decrease rate λ (Equation 2) step by step and then conducting the analysis.

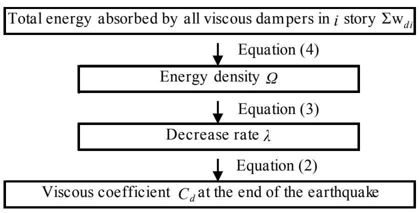

Figure 12 Flowchart for the simplified method

4.1 Analysis of Art-Hachi

The story drift angle R under Art-Hachi is presented in Figure 13. From Figure 13, it can be seen that $_{M}$R100、$_{L}$R100 schemes achieved R less than 1/100, and $_{M}$R150、$_{L}$R150 schemes achieve R less than 1/150.

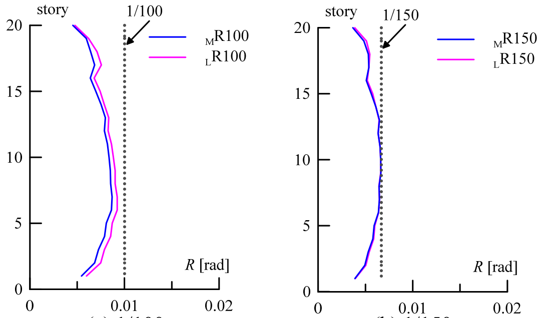

(a) 1/100 (b) 1/150

Figure 13 Story drift angle (Art-Hachi)

4.2 Analysis of Medium-sized Damper

Figure 14 presents the maximum story drift angle R, and the maximum absolute acceleration Acc. by the three analysis methods. From Figure 14(a), it can be seen that when the structure is elastic, the conventional method< detailed method < simplified method. The simplified method is the most effective amongst the three methods. The same tendency is evident in absolute acceleration Acc. From Figure 14(b), when the structure is elasto-plastic, with the same tendency as 14(a) is seen. However, when the structure is elasto-plastic, the absorbed energy of dampers decreased, the performance decrement is smaller than when the structure is elastic, and the difference between the three methods is smaller than in Figure 14(a).

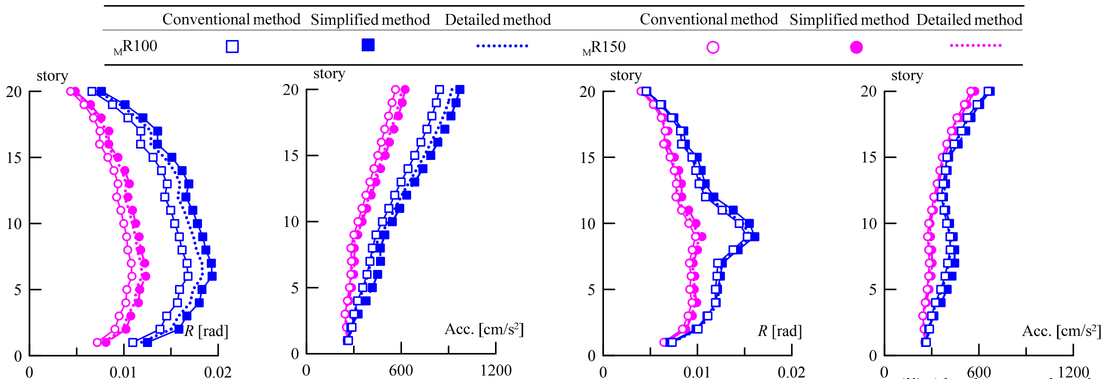

(i) Story drift angle (ii) Absolute acceleration (i) Story drift angle (ii) Absolute acceleration

(a) Elastic (b) Elasto-plastic

Figure 14 Medium-sized dampers (CH1)

4.3 Analysis of Large-sized Damper

Figure 15 presents the maximum story drift angle R, and absolute acceleration Acc. by the three analysis methods. From Figure 15, the same tendency as section 4.2 can be seen. From Figure 14 and Figure 15, the difference of the large-sized damper of the three methods is smaller than the medium-sized damper, the reason will be discussed later.

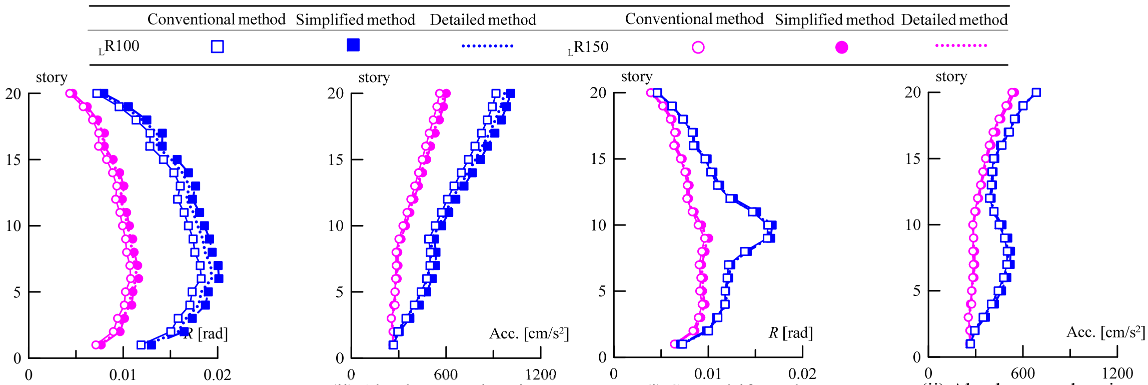

(i) Story drift angle (ii) Absolute acceleration (i) Story drift angle (ii) Absolute acceleration

(a) Elastic (b) Elasto-plastic

Figure 15 Large-sized dampers (CH1)

5 DECREASE RATE

5.1 Analysis of Energy

Figure 16 presents the absorbed energy of individual damper w_d in i story. From Figure 16(a), it is seen that when the structure is elastic, for $_{M}$R100 the simplified method < detailed method <conventional method. For $_{M}$R150, w_d is almost the same in each method. Moreover, w_d of $_{M}$R100 is greater than $_{M}$R150, as the volume of the viscous fluid V_V is the same, the performance decrement of $_{M}$R100 is greater than $_{M}$R150. The number of damper is larger, the performance decrement of the damper is less. In addition, it can be seen that w_d of the large-sized damper is greater than the medium-sized damper. From figure 16(b), when the structure is elasto-plastic, since w_d is smaller, the difference of each method is smaller than when the structure is elastic.

Figure 17-18 presents the damping energy of structure W_{fh}, the plastic energy of structure W_{fp} and the absorbed energy of total viscous dampers W_d. From Figure 17(a), for $_{M}$R100 because of the performance decrement, it is shown that the W_d of simplified method < detailed method < conventional method. For $_{M}$R150, as the performance decrement is small, W_d is almost the same in each method. Moreover, the W_d of $_{M}$R150> $_{M}$R100, so the number of damper is larger, and the W_d is more. In Figure 17(b), the same tendency as Figure 17(a) is seen. However, as the structure is elasto-plastic, W_d of $_{M}$R100 decreased significantly, but W_d of $_{M}$R150 is almost the same. In Figure 18, the same tendency as Figure 17 is seen. From Figures 17 and 18, it can be seen that the W_d of R150 is almost the same whether the structure is elasto-plastic or not. Moreover, the W_d of R150 is more than R100.

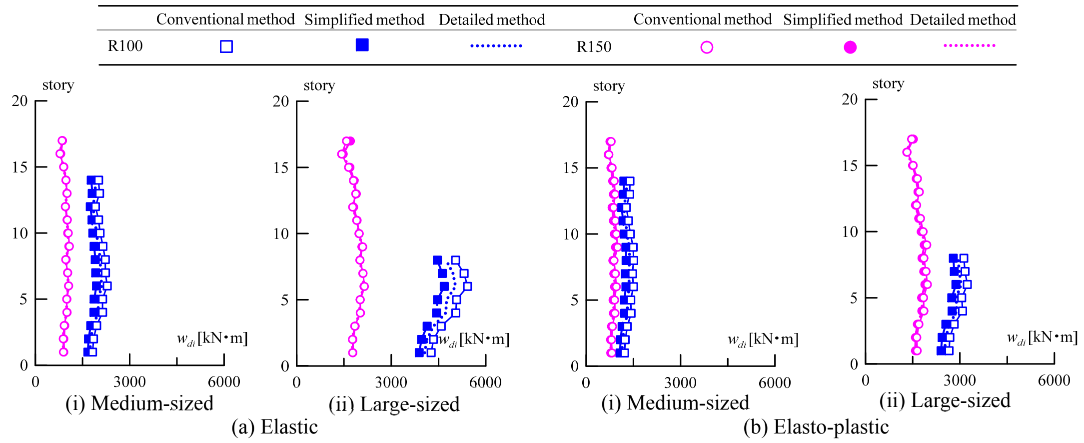

Figure 16 Energy absorbed by individual viscous dampers (CH1)

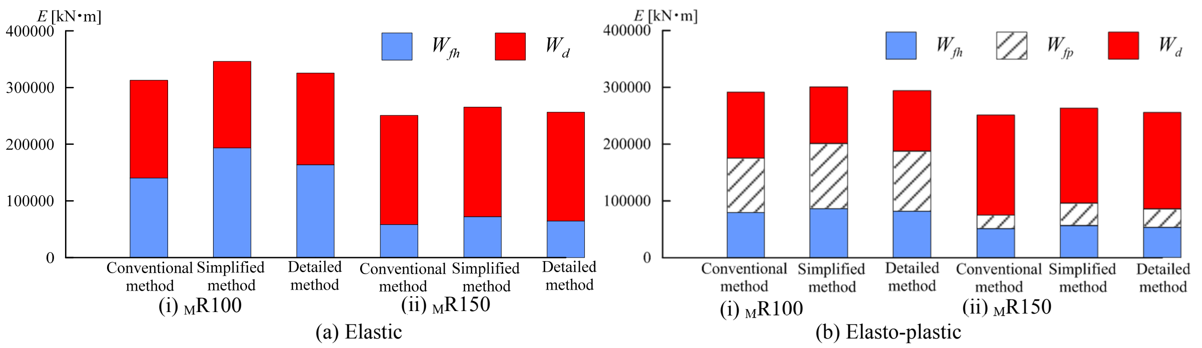

Figure 17 Distribution of the energy of medium-sized dampers

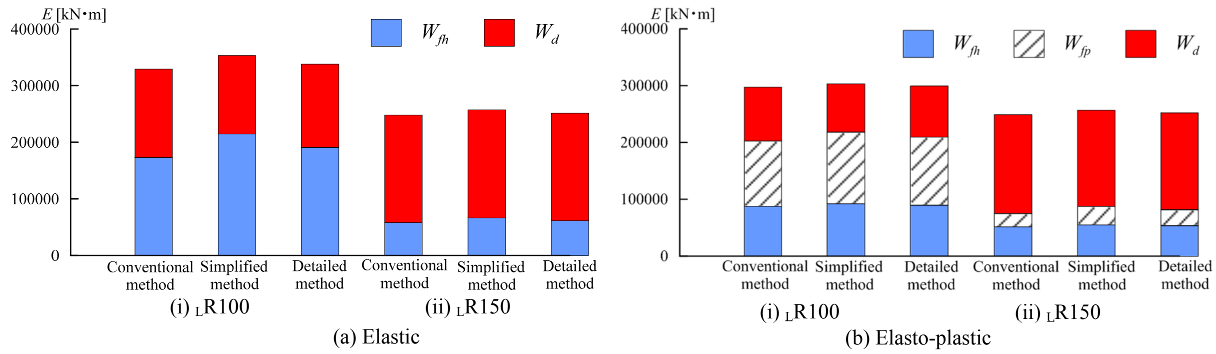

Figure 18 Distribution of the energy of large-sized dampers (CH1)

5.2 Decrease Rate by Two Types of Dampers

Figure 19 presents the absorbed energy of individual damper w_d in i story. In Figure 19(a), it is shown that w_d ($_L$R100) > w_d ($_M$R100)> w_d ($_L$R150)> w_d ($_M$R150). In Figure 19(b), it is shown that w_d ($_L$R100) > w_d ($_L$R150)> w_d ($_M$R100)> w_d ($_M$R150), that is because when the structure is plastic, the w_d of R100 decreased significantly. From Figure 19, it can be seen that in the same condition, w_d of large-sized damper > medium-sized damper and w_d of R100> R150.

Figure 20 presents the decrease rate λ defined by Esquation (3). From Figure 20, it can be seen that whether the structure is elasto-plastic or not, λ ($_L$R150) > λ ($_M$R150)> λ ($_L$R100)> λ ($_M$R100). In the same condition, w_d of large-sized damper > medium-sized damper, V_V of large-sized damper is 3 times larger than medium-sized damper, the performance decrement of medium-sized damper > large-sized damper. And when the number of damper is larger, the performance decrement is less. Moreover, it can be seen that since w_d of R100 decreased significantly, the λ of R100 increased while the λ of R150 is almost the same.

Figure 21 presents the hysteresis loop of individual damper of $_M$R100 in the 6th story under CH1. From figure 21, it can be seen that the performance decrement of simplified method > detailed method >conventional method. In addition, w_d of structure is elastic > plastic, which is the same as Figure 19.

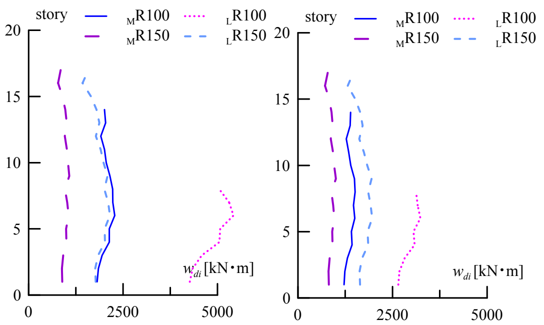

(a) Elastic (b) Elasto-Plastic

Figure. 19 Energy absorbed by individual dampers (CH1)

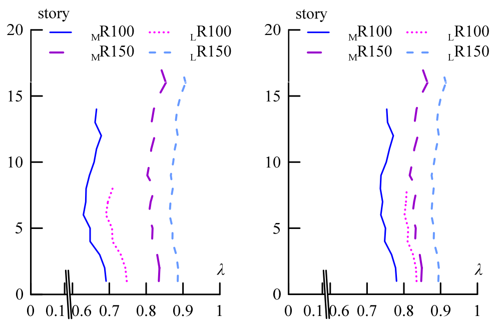

(a) Elastic (b) Elasto-Plastic

Figure. 20 Decrease rate of individual dampers (CH1)

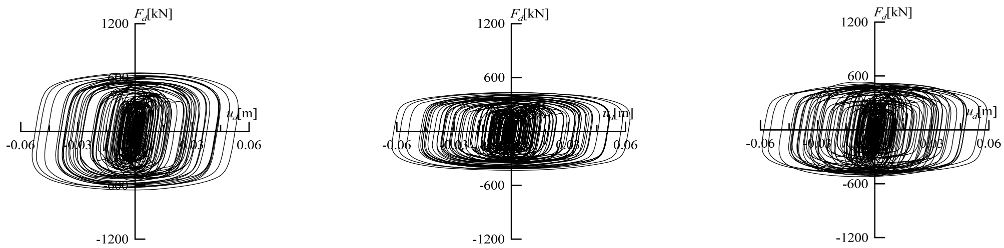

(i) Conventional method (ii) Simplified method (ii) Detailed method

(a) Elastic

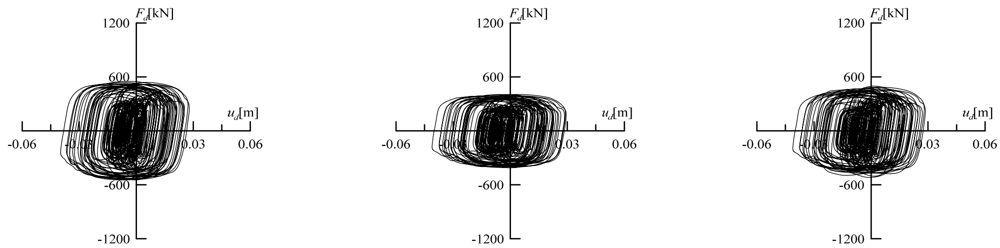

(i) Conventional method (ii) Simplified method (ii) Detailed method

(b) Elasto-Plastic

Figure 21 Hysteresis loop of $_M$R100 under CH1 (6th story)

5.3 Decrease Rate by Three Analysis Methods

Figure 22～23 presents the time history of the decrease rate λ of ${}_{M}R100$ and ${}_{L}R150$ at the same position in the 2nd and 6th stories. From Figure 23, it can be seen that λ changed each step by detailed method. In addition, λ of the 6th story is smaller than the 2nd story, as the story drift of the 6th story is larger than the 2nd story, the w_d is more. In addition, when the structure is elasto-plastic, as the absorbed energy of dampers decreased, the λ of ${}_{M}R100$ increases, and is the same as in Figure 20. From Figure 23, it can be seen that λ of ${}_{L}R150$ is almost the same whether the structure is elasto-plastic or not. In Figures 22 and 23, the λ of ${}_{L}R150$ is larger than ${}_{M}R100$.

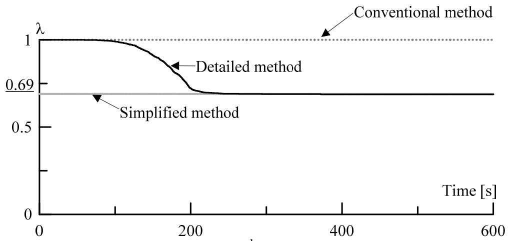

(i) 2nd Story

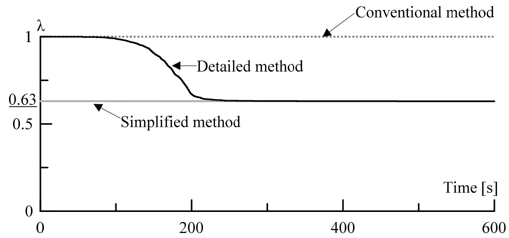

(ii) 6th Story

(a) Elastic

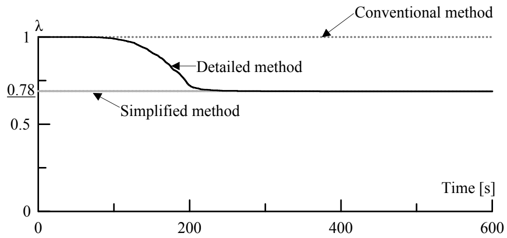

(i) 2nd Story

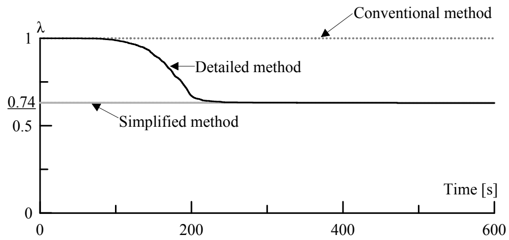

(ii) 6th Story

(b) Elasto-Plastic

Figure 22 Time history of decrease rate of ${}_{M}R100$ (CH1)

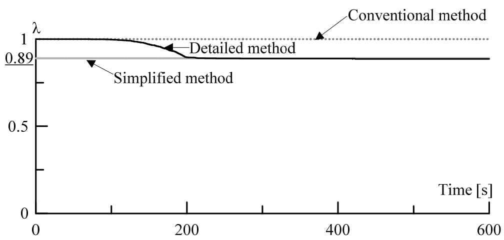

(i) 2nd Story

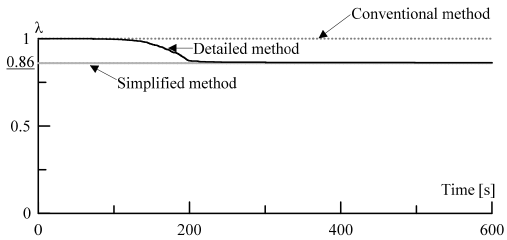

(ii) 6th Story

(a) Elastic

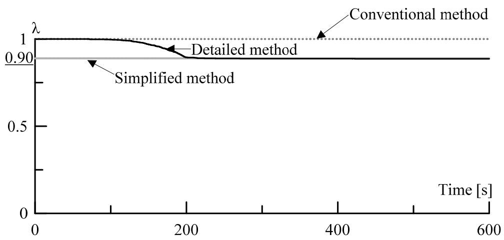

(i) 2nd Story

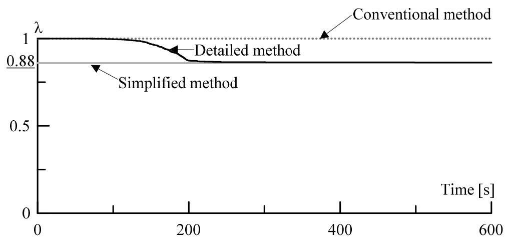

(ii) 6th Story

(b) Elasto-Plastic

Figure 23 Time history of decrease rate of ${}_{L}R150$ (CH1)

6 CONCLUSIONS

This paper presents the seismic response of a 20-story building with viscous dampers considering the performance decrement under long-period ground motion using a 3D model. The main structure is elastic and elasto-plastic. The viscous dampers are evaluated for two types of dampers, medium-sized dampers and large-sized dampers. The three analysis methods, the conventional method, simplified method, and detailed method, were also assessed. The following conclusions can be drawn:

(1) The simplified method is the most effective among the three methods in terms of design.

(2) The performance decrement of the large-sized damper is less than the medium-capacity damper whether the structure is elasto-plastic or not. It is better to use the large-sized damper for design.

(3) When the number of damper is larger, the performance decrement is the less whether the structure is elasto-plastic or not. Since the number of damper for story drift angle 1/150 is larger, it is better to use the story drift angle 1/150 for design.

ACKNOWLEDGMENT

This work was supported by the JST Program on Open Innovation Platform with Enterprises, Research Institute and Academia.

REFERENCES

[1] Akiyama, H., "Earthquake-Resistant Design Method for Buildings Based on Energy Balance," Gihodo Shuppan Inc., 1999. [*in Japanese*]

[2] Kasai, K., Sato, D., Matsuda, K., and Nagayama, S., "Variations in Synamiv Properties of Four Types of Full-scale Dampers Under Long-Duration Harmonic Loadig and Their Simplified Prediction Methods," *AIJ Journal of Structural Engineering*, 63B, 275-284,2017. [*in Japanese*]

[3] Nagayama, S., Sato, D., Kasai, K., and Matsuda, K., "Simplified Response Evaluation of Vibration Control Building with Viscous Dampers under Long Period Ground Motion, Part 2 : Response Evaluation Considering Change in Dynamic Properties of Viscous Damper," *AIJ Summaries of technical papers of annual meeting*, B-2, 165-166, 2017. [*in Japanese*]

[4] Nagayama, S., Sato, D., Kasai, K., and Matsuda, K., "Simplified Response Evaluation of Vibration Control Building with Viscous Dampers under Long Period Ground Motion, Part 4: Time History Response Analysis Results," *AIJ Summaries of technical papers of annual meeting*, Structure-II, 613-614, 2017. [*in Japanese*]

[5] Sato, D., Kasai, K., Nagayama, S., and Matsuda, K., "Response Evaluation Prediction of Passive Control Structure with Viscous Dampers Considering its Performance Decrement under Long-period Ground Motion," *40th IABSE Symposium*, S4,19-26, 2018

[6] Sato, D., and Okada, R., "Response Evaluation Methods for Passive Controlled Building with Viscous Dampers Considering its Performance Decrement against Long-period Ground Motion," *The 7th Asia Conference on Earthquake Engineering*, 2018

[7] Okada, R., Sato, D., and Liu, X., "Analysis on Energy of Passive Control Structure with Viscous Dampers (Part1: Response Evaluation Method of Viscous Dampers Considering its Performance Decrement)," *AIJ Summaries of technical papers of annual meeting*, 405-408, 2018. [*in Japanese*]

[8] Okada, R., and Sato, D., "Analysis on Energy of Passive Control Structure with Viscous Dampers (Part2: Prediction Accuracy of Absorbed Energy by Viscous Damper)," *AIJ Summaries of technical papers of annual meeting*, 409-412, 2018. [*in Japanese*]

[9] Architectural Institute of Japan (AIJ), "Recommended Provision for Seismic Damping Systems applied to Steel Structures", 2014. [*in Japanese*]

[10] Okada, R., and Sato, D., "Validity of Simplified Response Evaluation Method considering Performance Degradation of Viscous Dampers," *AIJ Summaries of technical papers of annual meeting*, 2018. [*in Japanese*]

[11] Building Research Institute (BRI), "The Main Point to Consider Long Period Ground Motion and the Concept of the Ground Motion," 2017